◆ Human Brain Mapping 35:2206–2219 (2014) ◆

The Role of Dysfunctional Attentional Control Networks in Visual Misperceptions in Parkinson's Disease

James M. Shine,[1] Glenda M. Halliday,[2,3] Moran Gilat,[1] Elie Matar,[1] Samuel J. Bolitho,[1] Maria Carlos,[1] Sharon L. Naismith,[1] and Simon J.G. Lewis[1]*

[1]Parkinson's Disease Research Clinic, Brain and Mind Research Institute, The University of Sydney, New South Wales, Australia
[2]Neuroscience Research Australia, Sydney, New South Wales, Australia
[3]The University of New South Wales, Sydney, New South Wales, Australia

Abstract: Visual misperceptions and hallucinations represent a problematic symptom of Parkinson's disease. The pathophysiological mechanisms underlying these symptoms remain poorly understood, however, a recent hypothesis has suggested that visual misperceptions and hallucinations may arise from disrupted processing across attentional networks. To test the specific predictions of this hypothesis, 22 patients with Parkinson's disease underwent 3T fMRI while performing the Bistable Percept Paradigm, a task that has previously been shown to identify patients with hallucinations. Subjects are required to study a battery of randomly assigned "monostable" and "bistable" monochromatic images for the presence or absence of a bistable percept. Those patients who scored a high percentage of misperceptions and missed images on the task were less able to activate frontal and parietal hubs of the putative Dorsal Attention Network. Furthermore, poor performance on the task was significantly correlated with the degree of decreased activation in a number of these hubs. At the group level, the difference between processing a bistable versus a monostable cue was associated with increased recruitment of the anterior insula. In addition, those patients with impaired performance on the paradigm displayed decreased resting state functional connectivity between hubs of the Ventral and Dorsal Attention Networks. These same patients had significantly decreased gray matter in the insula bilaterally. In addition, a combined analysis of the separate neuroimaging approaches revealed significant relationships across the impaired networks. These findings are consistent with specific predictions from a recently proposed hypothesis that implicates dysfunction within attentional networks in Parkinsonian hallucinations. *Hum Brain Mapp 35:2206–2219, 2014.*

Key words: functional magnetic resonance imaging; visual misperceptions; Parkinson's disease; bistable percept paradigm; hallucinations

Contract grant sponsors: Australian Rotary Health Scholarship, NHMRC Postgraduate Scholarship, University of Sydney Rolf Edgar Lake Postdoctoral Fellowship; Contract grant sponsor: Senior Principal Research Fellowship of the NHMRC; Contract grant number: 630434; Contract grant sponsor: NHMRC Career Development; Contract grant number: 1008117; Contract grant sponsor: NHMRC Practitioner Fellowship; Contract grant number: 1003007

*Correspondence to: Simon J.G. Lewis, Parkinson's Disease Research Clinic, 94 Mallett Street, Camperdown, Sydney, New South Wales 2050, Australia. E-mail: simonl@med.usyd.edu.au

Received for publication 11 December 2012; Revised 1 April 2013; Accepted 15 April 2013.

DOI: 10.1002/hbm.22321
Published online 13 June 2013 in Wiley Online Library (wileyonlinelibrary.com).

INTRODUCTION

Visual misperceptions and hallucinations (VH) occur in over half of all patients with Parkinson's disease (PD), particularly in the latter stages of the condition [Diederich et al., 2009; Fenelon et al., 2000; Forsaa et al., 2010; Sanchez-Ramon et al., 1996]. These symptoms often occur along a distinct spectrum, with visual misperceptions representing the incorrect recognition of a perceived stimulus and hallucinations representing the occurrence of a perception in the absence of a clear stimulus. Despite their negative impact on patient outcomes [Goetz et al., 2006], these neuropsychiatric symptoms remain poorly understood in PD, with limited therapeutic options [Diederich et al., 2009; Forsaa et al., 2010; Sanchez-Ramon et al., 1996].

Although the pathophysiology of VH is poorly understood, a number of theories have been proposed as explanations for VH in PD. For instance, the presence of VH in clinical disorders that effect the retina, such as Charles Bonnet Syndrome [Berrios, 1982], has led to the proposal that the VH suffered in PD may result from impairments within the visual pathway. Indeed, both reduced contrast and color discrimination have been reported in PD patients with hallucinations and may relate to a primary loss of dopaminergic retinal cells [Pieri et al., 2000]. Additionally, it is well recognized in clinical practice that reduced ambient lighting and unfamiliar environments are associated with increased perceptual errors. This has led to the proposal that these visual impairments may induce a partial sensory deprivation that permits the emergence of previously recorded percepts, which then form the basis for VH [Diederich et al., 1998].

In addition to the potential role of retinal pathology, structural neuroimaging studies have confirmed atrophy across limbic neural regions in hallucinating PD patients [Ibarretxe-Bilbao et al., 2010, 2011; Janzen et al., 2012] as well as in frontal and visual association regions [Ramírez-Ruiz et al., 2007; Sanchez-Castaneda et al., 2010]. The latter results are consistent with recent work utilising functional Magnetic Resonance Imaging (fMRI), which demonstrated reduced activation in occipital and temporal cortices in PD patients with VH when presented with visual stimuli [Meppelink et al., 2009]. A separate fMRI study has demonstrated that PD patients with chronic VH respond to the presentation of simple visual stimuli with greater frontal and caudate nucleus activation and less visual cortical activation than non-hallucinating PD subjects [Stebbins et al., 2004]. This finding suggests that impaired processing of visual information may trigger "higher order" frontal regions. However, a subsequent fMRI study utilising the presentation of more complex visual stimuli failed to find any evidence to support this "top-down" compensatory process [Meppelink et al., 2009]. In addition to the results of these neuroimaging studies, a strong clinicopathological correlation has been found between VH and Lewy body (LB) pathology within temporal cortical structures, such as the amygdala and parahippocampal gyrus [Harding et al., 2002], suggesting that VH in PD relate to a disruption across diverse yet related neural circuitry.

These findings have led to several separate proposals suggesting that hallucinations in PD are related to deficits in perception and attention [Bronnick et al., 2005; Collerton et al., 2005; Diederich et al., 2005; Gallagher et al., 2011; Pieri et al., 2000; Price et al., 1992] being modulated by both neurotransmitter disturbances [Goetz et al., 1982, 1998] and specific subcortical and cortical pathology [Harding et al., 2002; Ramírez-Ruiz et al., 2007; Sanchez-Castenada et al., 2010; Janzen et al., 2012]. In an attempt to integrate these processes, a recent attentional network hypothesis has proposed that VH in PD may arise from dysfunction across the attentional control networks comprising the dorsal attention network (DAN), the ventral attention network (VAN), and default mode network (DMN) [See Table I; Shine et al., 2011]. Specifically, this model proposes that VH are due to a relative inability to recruit activation in the DAN in the presence of an ambiguous percept, leading to an "over reliance" on the VAN and DMN. The DAN, which underlies the capacity to focus attention on externally driven percepts, is comprised

TABLE I. Attentional control networks

Network	Anatomical areas	Function
Default Mode Network (DMN)	• Medial temporal cortex • Medial PFC • Posterior cingulate	• Task-independent introspection • Self-referential tasks
Dorsal Attentional Network (DAN)	• Dorsolateral PFC • Posterior parietal cortex • Frontal eye fields • Corpus striatum	• Voluntary orienting • Cognitive information processing
Ventral Attentional Network (VAN)	• Basolateral amygdala • Lateral and inferior PFC • Temporoparietal junction • Ventral striatum	• Mediate activation of other networks • Engages attention to salient stimuli

PFC, prefrontal cortex.

of widespread neural regions within the frontal eye fields, the dorsolateral prefrontal cortex and the superior posterior parietal cortices, all of which send efferents to the head of the caudate nucleus [Asplund et al., 2010]. The model proposes that an inability to recruit this network would lead to an over-reliance on the VAN, which normally assists in the rapid re-orienting of attention towards salient stimuli [Corbetta and Shulman, 2002] and the DMN, which consists of regions normally involved in the retrieval and manipulation of episodic memories and semantic knowledge [Binder et al., 1999; Mazoyer et al., 2001; Spreng et al., 2010].

The attentional network hypothesis of VH has received preliminary supportive evidence through behavioral testing using the novel Bistable Percept Paradigm [BPP; Shine et al., 2012]. The BPP is a computer-based task that requires participants to evaluate a battery of monochromatic "monostable" and "bistable" percepts and impaired performance on this task distinguishes those PD patients who experience VH [Shine et al., 2012]. A similar approach has also recently been utilized to demonstrate complex visual illusions in patients with Dementia with Lewy bodies [Uchiyama et al., 2012]. An increased percentage of mistakes on the BPP was associated with specific impairments in attentional set-shifting ability, implicating an inability to effectively recruit the DAN in PD patients with VH. Furthermore, a recent MR spectroscopy (MRS) study found that the severity of impairments on the BPP was associated with reduced neuronal integrity (as measured by the ratio of *N*-Acetyl Cysteine to Creatine) in the anterior cingulate cortex, a neural hub with connections to a number of different attentional networks [Lewis et al., 2012].

In the current study, we sought to further assess the attentional network hypothesis using a number of different MRI-based imaging modalities, including event-related fMRI, resting state functional connectivity MRI (rsfcMRI) and structural neuroimaging using voxel-based morphometry (VBM). We hypothesized that impaired performance on the BPP in those patients with VH would be associated with reduced activation patterns across the DAN and structural changes within neural regions that are known to be critical for integration across the attentional networks.

METHODS

Participants

The 22 patients with PD included in this study were all recruited from the Brain and Mind Research Institute Parkinson's Disease Research Clinic. All patients satisfied the United Kingdom Parkinson's Disease Society (UKPDS) Brain Bank criteria, showed no signs of overt dementia [Martinez-Martin et al., 2011] and were assessed on their regular medication. Demographic details are presented in Table II. Permission for the study was obtained from the local research ethical committee and all patients gave written informed consent.

TABLE II. Demographic and neuropsychological characteristics

	Non-hallucinators	Hallucinators	*P* value
Number	13	9	
Age	61.5 ± 5.5	65.7 ± 4.1	ns
Disease duration (years)	4.9 ± 2.9	6.7 ± 3.2	ns
UPDRS III[a]	21.1 ± 9.1	27.6 ± 14.2	ns
Hoehn and Yahr, stage	2.1 ± 0.4	2.1 ± 0.2	ns
Dopa dose equiv, mg/day[a]	1264.0 ± 517	1081.9 ± 680	ns
BDI-II[a]	8.0 ± 7.4	9.2 ± 6.1	ns
MoCA	27.1 ± 2.1	26.7 ± 2.1	ns
TMT_{B-A}[a]	48.5 ± 47.6	89.6 ± 29.8	< 0.05
$SCOPA\text{-}PC_{1-4}$[a]	0.5 ± 0.7	2.6 ± 1.9	< 0.01
RBD-Q[a]	4.5 ± 3.7	7.4 ± 2.2	< 0.05
BPP error score (%)[a]	9.1 ± 3.8	19.4 ± 6.8	< 0.05
Contrast sensitivity	1.69 ± 0.0	1.60 ± 0.0	ns

UPDRS, Unified Parkinson's Disease Rating Scale; BDI, Beck's Depression Inventory; MoCA, Montreal Cognitive Assessment; TMT_{B-A}, Trail Making Test: Part B minus Part A; RBD-Q, Rapid Eye Movement Behavior Disorder Questionnaire; BPP, Bistable Percept Paradigm.
[a]*t*-Test with unequal variance.

All patients underwent assessment in their "on" state. The patients were all rated as between Hoehn and Yahr stages I–IV and were assessed on section III of the Unified Parkinson's Disease Rating Scale [UPDRS-III; Goetz et al., 2007]. Two patients were taking dopamine agonist monotherapy, one patient was untreated and the other nineteen were taking levodopa: six of whom were on levodopa monotherapy; two who were taking adjuvant entacapone; five who were taking a combination of levodopa and dopamine agonist therapy and six who were on a combination of levodopa, entacapone, and a dopamine agonist. Two patients were taking a selective serotonin reuptake inhibitor for mood and one patient was taking a nocturnal benzodiazepine to aid sleep. Dopamine dose equivalence scores were also computed for each patient. While it is well known clinically that visual misperceptions are worsened by dopaminergic medication, patients were studied in the "on" state in order to accurately reflect their regular daily functioning. In addition, none of the patients self-reported severe hallucinations and as such, were not contraindicated from taking dopamine agonist therapy.

All of the participants underwent two tests of visual function. A Snellen chart test was administered to assess visual acuity and the Pelli-Robson test was administered to assess contrast sensitivity [Elliot et al., 1990]. Patients were all tested in the same clinical environment with consistent artificial lighting. If required, patients were allowed to wear MRI-safe spectacles in order to correct visual

deficits and the visual acuity testing described above occurred while wearing these goggles.

Neuropsychological Assessments

Performance data is included in Table II. None of the patients showed evidence of clinical dementia [Emre et al., 2007]. The Montreal Cognitive Assessment (MoCA) was used as general measure of cognition [Gagnon et al., 2010] and the Beck Depression Inventory (BDI-II) was utilized to assess for the presence of affective disturbance [Beck et al., 1996]. Sleep quality was assessed using the Rapid Eye Movement Sleep Behavioral Disorder Questionnaire [Scaglione et al., 2005] as these symptoms have been shown to be strongly associated with the presence of hallucinations [Nomura et al., 2003]. To explore the role of attentional set-shifting, all patients performed the Trail Making Test (TMT) parts A and B [Corrigan and Hinkeldey, 1987], allowing for the calculation of a difference score (TMT_{B-A}) [Naismith et al., 2010]. All behavioral data analysis was performed using SPSS version 20 (Chicago, IL, USA).

Bistable Percept Paradigm (BPP)

The BPP consisted of a battery of monochromatic black and white images that contained with a series of monochromatic black and white images, which were classified a priori as either monostable or bistable images [Shine et al., 2012]. As shown in Figure 2, bistable images were like the classic "faces in profile or vase" whereas monostable images had no such ambiguity. The paradigm was constructed using EPrime Software (Psychology Software Tools, USA) and all patients were trained on a sample of the paradigm before commencing the study. The experimental trial was conducted with the patient lying in a 3 Tesla MR scanner with the task displayed on a screen in the patient's direct line of vision. While lying in the scanner, the patient's left and right hands were positioned over corresponding response buttons that controlled both the initial response to the cue as well as to the answers of subsequent questions [Shine et al., 2012]. Stimulus images from the training period were not presented during the MRI scanning task.

Each trial was signaled by the appearance of a black fixation crosshair in the middle of a white screen. After a delay of 50 ms, the crosshair disappeared and participants were randomly presented with one of the images. Subjects were required to study the image until they were satisfied that they had recognized everything that the image may represent (i.e., decide whether they were perceiving either a monostable or bistable percept) before pressing a response button. This response triggered a screen where participants indicated by button press whether they had identified a monostable or bistable percept by pressing the associated button. Following this button-press, the fixation crosshair re-appeared signaling the start of the next trial. This method allowed for a predictable pattern of presentation and questioning, however, the variable amount of time taken by each patient for viewing images and answering the relevant questions meant that the individual epochs associated with each image were randomly spread across the TR, allowing for adequate sampling of the BOLD response.

After demonstrating familiarity with the BPP on a laptop computer in a clinical environment, subjects performed two separate trials of the paradigm in the MRI scanner, each including a sample of 40 monostable images and 40 bistable images. Button responses were logged during the experimental paradigm, determining whether an individual patient had experienced either a monostable or bistable percept. Following the experiment, a member of the research team interviewed each patient while they reviewed all 80 items and described the specific images that they saw in each percept aloud to the examiner. If there was a discrepancy, trials were scored according their responses at the postscanning debrief session.

The program logged both the specific time point (in seconds) when each patient pushed the response button as well as whether the percept viewed was thought to represent a monostable or bistable percept. This allowed for the post hoc calculation of a number of outcome measures, including: correct responses on monostable images; correct responses on bistable images; missed images, which reflected the mislabeling of a bistable image as a monostable percept; and misperceptions, which reflected the incorrect identification of a monostable image as a bistable percept or incorrectly reporting a perception that was not present in either the monostable or bistable image.

BPP Error Score

Using a larger cohort of patients with PD and healthy age-matched controls, we have previously demonstrated the utility of the BPP in accurately classifying patients as either "BPP impaired" (i.e., patients with a high proportion of mistakes, such as misperceptions) or "BPP normal" (i.e., minimal mistakes on the paradigm) [Shine et al., 2012; Lewis et al., 2012]. In a similar manner to the previous study, an error score was calculated by averaging the percentage of missed images and Misperceptions and using the same error "cut-score" (derived from the previous testing of an age-matched control group), we were able to classify patients as "BPP impaired" or "BPP unimpaired".

To confirm the presence of visual misperceptions in the BPP impaired cohort, the inclusion of each patient into either group was compared to each patient's response to the second question of the MDS-UPDRS, a measure that has previously been used to effectively screen for the presence of visual hallucinations in PD [Llebaria et al., 2010]. There was a direct concordance between the two measures, as each patient that scored a "1" or greater on the second

question of the MDS-UPDRS was labeled as a "hallucinator" after a selection that was based on the BPP Error score (five patients scored 1, three patients scored 2 and one scored 3). Each patient who scored "0" was labeled as a "non-hallucinator." In addition, each patient completed the first four questions from the Scales for Outcome in PD-Psychiatric Complications (SCOPA-PC), which explicitly questions for the presence of visual misperception and hallucinations, as well as probing for the presence of delusional thinking [Visser et al., 2007]. Each patient from the "hallucinator" group scored positively on this questionnaire. After separating the PD patients into two groups based on their BPP error score, independent-sample *t*-tests were used to test for differences between the two groups.

Neuroimaging Analysis

Image acquisition

Imaging was conducted on a General Electric 3 Tesla MRI (General Electric, Milwaukee, USA). T2*-weighted echo planar functional images were acquired in sequential order with repetition time (TR) = 3 s, echo time (TE) = 32 ms, flip angle = 90◦, 32 axial slices covering the whole brain, field of view (FOV) = 220 mm, interslice gap = 0.4 mm, and raw voxel size = 3.9 mm by 3.9 mm by 4 mm thick. T1-weighted images were also acquired, consisting of a set of 126 adjacent axial cuts parallel to the anterior commissure-posterior commissure line, with a slice thickness of 1.5 mm and a voxel size of $1 \times 1 \times 1$ mm^3. A separate resting state trial was collected following the performance of the BPP, consisting of 140 scans collected with the same parameters as the functional trials. During this trial, patients were asked to lie still with their eyes closed and to let their minds wander freely.

Image preprocessing

Statistical parametric mapping software (SPM8, Wellcome Trust Centre for Neuroimaging, London, UK, http://www.fil.ion.ucl.ac.uk/spm/software/) was used for image processing and analysis. Functional images were preprocessed according to a standard pipeline: (a) scans were slice-time corrected to the median (17th) slice in each TR; (b) scans were then realigned to create a mean realigned image and measures of 6 degrees of rigid head movements were calculated for later use in the correction of minor head movements; (c) due to the increased risk of head movements in this clinical population, each trial was subsequently analyzed using ArtRepair [Mazaika et al., 2005] and trials with a large amount of global drift or scan-to-scan head movements greater than 1 mm were corrected using interpolation. Trials with head-movements greater than 3 mm or 3 degrees of movement were removed from the analysis; (d) images were normalized to the Echo Planar Image (EPI) template; (e) scans were then smoothed using an 8-mm full-width half-maximum isotropic Gaussian kernel

Event-related functional MRI analysis

Statistical parametric maps were calculated for each subject using a general linear model analysis within an event-related design. The onset and duration of each monostable image and each bistable image were modeled separately in each individual patient's first level design matrix. After estimation, this lead to the examination of the following specific contrasts: a comparison between the viewing of a monostable image against the global mean; a comparison between the viewing of a bistable image against the global mean; and a comparison between the pattern seen during bistable images and that seen during monostable images. Contrast images from the first-level analyses were then entered into a second-level random-effects design in order to determine the group-level effects of the condition of interest. We explored both the group-level patterns (using a one-sample *t*-test) as well as the group-level differences (using a two-sample *t*-test) between non-hallucinators and hallucinators. Data were initially analyzed with a height threshold of $P < 0.05$ (corrected for multiple comparisons using false detection rate) and an extent threshold of 10 voxels (per cluster). Due to the exploratory nature of the study, if no voxels survived the correction for multiple comparisons, the threshold was increased to $P < 0.001$ with a minimum cluster size of 10 for further exploration, however, inference was only made on these results if they were consistent with the results from the regions-of-interest (ROI) in the following section, which were defined a priori.

Region of interest analysis

To further explore the patterns of BOLD response across the attentional control networks, contrast images from the first-level analysis were subsequently analyzed using a set of a priori ROIs. This technique allowed for the systematic exploration of the imaging data within small, predefined volumes of the brain and also ensured that sole inference was not made from a large number of uncorrected statistical tests. Using the MarsBar toolbox in SPM8 [Brett et al., 2002], spherical ROIs were drawn around the peak voxels from the VAN (Anterior Insula (AI)): +/−42, 24, −20; and the dorsal anterior cingulate cortex (dACC): +/−12, 26, 28), the DAN (Superior Parietal Lobule (SPL): +/−27, −52, 57; and the frontal eye fields (FEF): +/−25, −8, 54) and the DMN (Hippocampal formation (HF): +/−22, −22, −22; and the anterior interparietal lobule (aIPL): +/−52, −48, 48), based on previously reported voxels' co-ordinates for these ROIs [Fox et al., 2005; Spreng et al., 2010].

The MarsBar toolbox was then used to extract contrast values for each ROI dependent on the contrast of

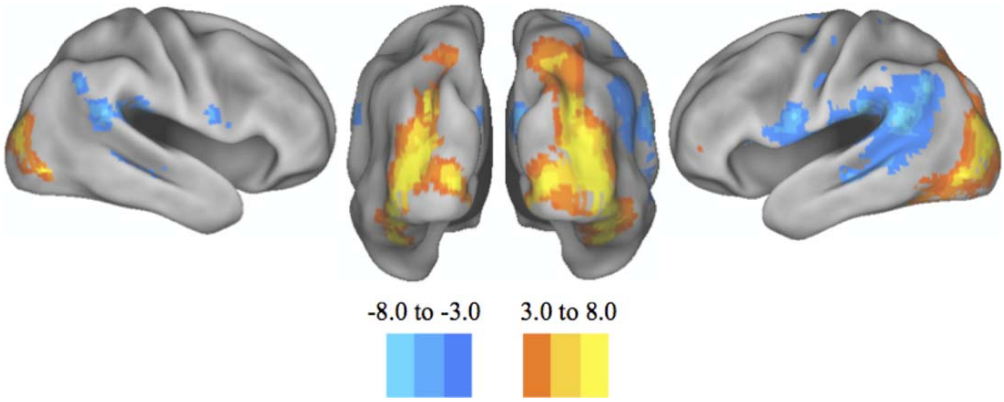

Figure 1.

Group similarities. Posterior and lateral views of the cortical surface rendering of the major areas of increased and decreased BOLD response during the processing of a visual cue. A similar pattern was seen when comparing the entire groups' response to the amalgamation of bistable and monostable images. Namely, there was a significant increase in the BOLD response within the bilateral occipital cortices, along with a decrease in the BOLD response in the bilateral temporoparietal junction. These results were significant after correction for multiple comparisons using a false detection rate of $P < 0.05$. [Color figure can be viewed in the online issue, which is available at wileyonlinelibrary.com.]

interest. These contrast values were then exported into SPSS for group-level testing, which involved both testing between groups using a two-sample *t*-test as well as correlating each contrast value with the percentage of misperceptions on the BPP using a Pearson's product-moment correlation. To assess the relative activity within each putative attentional network, the average contrast value for each network was calculated for each patient. This was calculated by averaging the contrast value for each of the hubs within a network, allowing for the comparison of group differences in the BOLD response within the different neural networks. While this method conveys some information about the patterns of coordinated activity within attentional networks, it does not allow any inference about the temporal relationships within these networks [Sporns, 2011].

Resting state functional connectivity analysis

In order to determine whether the regions identified in the functional analysis formed consistent functional networks, rsfcMRI analyses were applied to task-independent T2* data. rsfcMRI explores the temporal correlation between the BOLD response in different regions of the brain in the absence of any overt task [Van den Heuvel and Hulshoff Pol, 2010]. The degree to which disparate regions show increased rsfcMRI coherence has been taken to reflect the level and amount of information shared by the two hubs rather than their direct structural connection per se [Honey et al., 2009; Horwitz et al., 2005]. Previous neuroimaging studies assessing attention have shown increased coherence between the hubs comprising the putative VAN and the DAN [see above for ROI co-ordinates; Cortbetta and Shulman, 2002; Spreng et al., 2010].

Following the same preprocessing steps outlined for the functional experiment, images were imported into the Functional Connectivity ("conn") toolbox (http://www.nitrc.org/ projects/conn) in SPM8 for further data correction. After discarding the first five scans, the preprocessing steps included: (a) the application of a temporal band pass filter (0.009–0.08 Hz); and (b) the regression of nuisance parameters (and their first temporal derivative), including the six motion parameters extracted from realignment, the mean whole-brain signal and the signal from the voxel-stripped white matter and cerebrospinal fluid masks. The mean BOLD signal time course was then extracted from each of the ROIs from the functional analysis. The time course of each ROI was then correlated with the time course for each of the other ROIs, allowing for the calculation of a correlation coefficient for each ROI using a Pearson's product-moment calculation. These values were then converted into *Z*-scores using a Fisher's *r*-to-*Z* transformation, allowing for the calculation of the significant group similarities as well as the significant differences between the two groups ($P < 0.05$ FDR).

Voxel-based morphometry (VBM) analysis

To assess for any significant structural differences between the two groups of patients, individual T1-weighted images for each patient were subjected to VBM analysis using the SPM8 software package [for detailed methods, see Ashburner and Friston, 2000]. First, each T1 image was re-oriented to standard space. Following this, each image was segmented using the Segment tool in

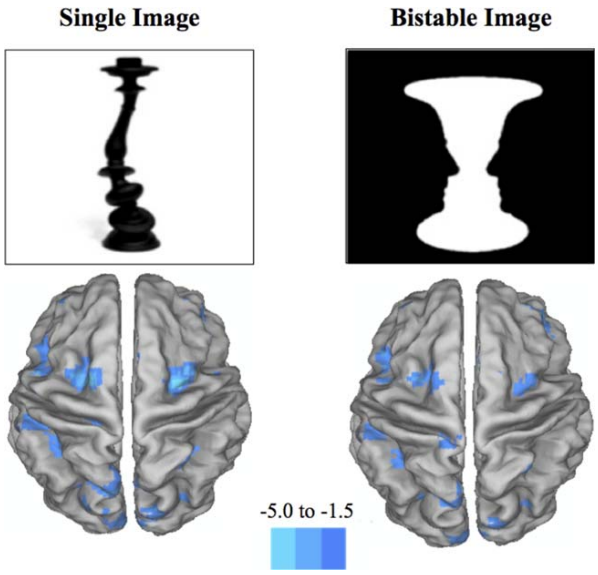

Figure 2.
Differences between two groups. Graphical depictions of the brain representing the main regions of increased BOLD contrast in the comparison of hallucinators against non-hallucinators ($P < 0.001$ and clusters = 10). The leftmost image represents the group differences when viewing bistable images and the rightmost image represents the differences when viewing a monostable image. The major differences were found in regions comprising the dorsal attention network, such as the bilateral frontal eye fields, the superior parietal lobule and the MT+ region. The blue color intensity in the image reflects the *t*-statistic from the second level random-effects comparison of hallucinators and non-hallucinators. [Color figure can be viewed in the online issue, which is available at wileyonlinelibrary.com.]

SPM8, which led to the creation of a gray matter template for each individual patient. These templates were then normalized to the 152MNI T1 template brain and then modulated, which involved scaling the gray matter template by the amount of contraction during spatial normalization, ensuring that the final gray matter template contains the same total amount of original gray matter as was present in the original image. Each image was then smoothed with an 8 mm FWHM Gaussian kernel. The smoothed images were subsequently entered into a second-level design, which compared hallucinators with non-hallucinators. Following this, the images were corrected for multiple comparisons using a False Detection Rate of $P < 0.05$. We then created a bilateral anterior insula mask, which contained each voxel from the VBM analysis that was significantly different between the two groups. This allowed for the calculation of the volume of gray matter within the bilateral AI for each individual patient, allowing for the subsequent correlation with the BPP Error score.

Inter-relation of task-based, rsfcMRI, and VBM analyses

To explore the data for the presence of inter-related signals within the three separate analytic techniques, the significant results from each of the previous three analyses were compared using Pearson's product-moment correlations. As in the previous analyses, alpha levels were set at $P < 0.05$.

RESULTS

Demographic Information

Of the 22 patients tested, the BPP identified 9 hallucinators and 13 non-hallucinators. As shown in Table II, the patient groups did not differ in age, disease duration, motor severity (UPDRS III score), Hoehn & Yahr stage, global cognition (MoCA), depressive symptoms or dopamine dose equivalence. In addition, there were no between-group differences in visual acuity or contrast sensitivity. In keeping with a previous study [Shine et al., 2012], there were strong inter-relationships between the measures of attentional-shifting (TMT_{B-A}) and the $SCOPA-PC_{1-4}$ ($r = 0.530$, $P < 0.01$) as well as the BPP error score ($r = 0.547$, $P < 0.01$).

Bistable Percept Paradigm

The average response time to process an image was 7.14 s. While the entire group of patients was more likely to take longer to identify the items within a monostable image ($t = 3.08$, $P < 0.01$), there were no significant differences between the two groups in the response time to either monostable ($t = 1.46$, $P = 0.159$) or bistable images ($t = 0.92$, $P = 0.370$).

Imaging Results

Group level similarities

In order to determine whether all patients recruited a similar network of visually-related neural regions during the processing of ambiguous visual images, we assessed the cortical BOLD response pattern associated with processing either a bistable or monostable image during performance of the BPP (Fig. 1). As predicted from the visual nature of the experimental paradigm, the cohort of PD patients showed a significant increase in the BOLD signal within the bilateral visual cortices. In addition, there was a significant decreased BOLD signal in the temporoparietal junction, bilaterally.

Group level differences

We subsequently analyzed the differences between the two groups of patients when they viewed both monostable

TABLE III. Brain regions displaying decreased BOLD response in both monostable bistable images (non-hallucinators versus hallucinators)

Neural region	*x*	*y*	*z*	Monostable cluster size	Bistable cluster size
Left frontal eye fields[a]	−27	0	64	129	64
Right frontal eye fields[a]	30	2	56	91	17
Midbrain	−2	−20	−6	91	139
pre-SMA[a]	0	20	46	77	56
L superior parietal lobule[a]	−22	−53	56	38	38
R superior parietal lobule[a]	22	−44	−18	11	32
Right visual area V2	11	−90	11	19	10

MNI co-ordinates for neural regions that displayed decreased BOLD response in the contrast between hallucinators and non-hallucinators when viewing both monostable and bistable images. The coordinates represent the peak voxel within a cluster that was present above the statistical threshold in both the monostable and the bistable contrast. T-statistics are presented for clusters with $P < 0.001$ and greater than 10 contiguous voxels corrected at the whole-brain level with a false detection rate of $P \leq 0.05$.
[a]Known hub of the Dorsal Attention Network.

and bistable images using a random-effects design (see Fig. 2). As predicted, there were a number of regions with significantly decreased BOLD recruitment when comparing hallucinators with non-hallucinators. When viewing either a monostable or a bistable image, hallucinators were significantly less able to recruit key regions within the DAN, including the bilateral frontal eye fields (peak voxel from the left hemisphere: −27, 0, 64; and right hemisphere: 30, 2, 56), the bilateral dorsolateral prefrontal cortex (left: −51, 29, 25 and right: 45, 35, 18), the bilateral superior parietal lobule (left: −22, −53, 56 and right: 22, −44, 58), the caudal midbrain (−2, −20, −6), the midline presupplementary motor area (0, 20, 46) and a region in the right parieto-occipital cortex (11, −90, 11). See Table III for the Cluster sizes in each contrast.

Data from the between-group analysis were then explored further using a series of a priori ROIs, each representing a key hub within the putative attentional control networks. Whilst both groups showed a consistent pattern of decreased DMN and VAN activity when assessing monostable and bistable contrasts (Fig. 3), hallucinators were unable to recruit activation in the DAN in the presence of either image (monostable: $t = 2.20$ and $P = 0.02$; bistable: $t = 2.52$ and $P = 0.01$). Across the whole cohort of patients, a relative increase in the amount of BOLD activity within the right frontal eye field ROI was negatively correlated with the percentage of misperceptions in both the monostable (Pearson's $r = -0.470$ and $P = 0.027$) and bistable ($r = -0.599$ and $P = 0.003$) percepts.

When analyzed as a single cohort, there was a significant group-level increase in the BOLD response within the left anterior insula (peak voxel: −25, 21, −9) in the bistable > monostable contrast. There were no significant

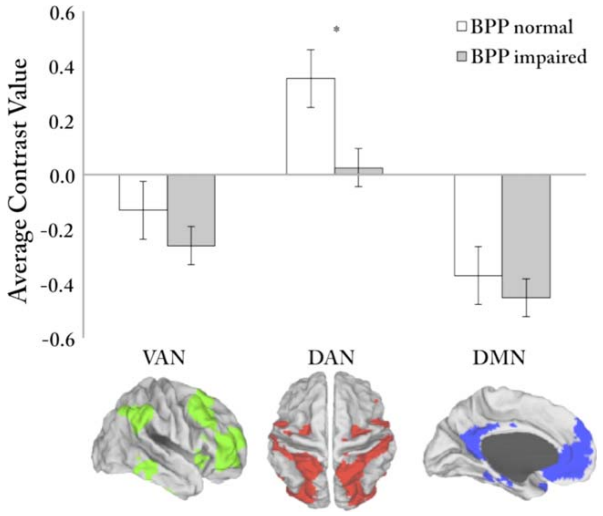

Figure 3.
Results of the region-of-interest analysis. Results from the direct comparison of the average contrast values from the attentional networks when comparing non-hallucinators (white columns) with hallucinators (gray columns) during the viewing of a bistable image. The contrast value represents the average value seen in each network during both monostable and bistable images. While there were no significant differences between patients in the VAN or DMN, hallucinators were significantly more likely to have a negative average contrast value in the DAN. Key: L, left; R, right; VAN, ventral attention network; DAN, dorsal attention network; DMN, default mode network. Significance levels: $*P < 0.05$. Though not explicitly shown here, the results were similar for the viewing of a monostable image. [Color figure can be viewed in the online issue, which is available at wileyonlinelibrary.com.]

differences between the two groups when comparing the unique response to bistable versus monostable images, either at the whole brain level or when constraining the analysis to the ROIs, however, this negative finding may be due to the relatively low sample size used in this experiment. This interpretation is in keeping with further analysis, as there were significant differences between the performance of bistable and monostable contrasts within the group of hallucinators. Specifically, the left dorsal anterior cingulate (average contrast value = 0.11; $t = 2.87$; $P = 0.02$) within the VAN and the left hippocampal formation (average contrast value = 0.12; $t = 2.62$; $P = 0.03$) within the DMN, were associated with a significantly increased BOLD response when viewing a bistable image.

rsfcMRI analysis

Both groups of patients displayed strong intra-network coherence in both the VAN and the DAN ($r > 0.15$ and $P < 0.05$), suggesting that each network contained high intra-network connectivity. Comparison between the two

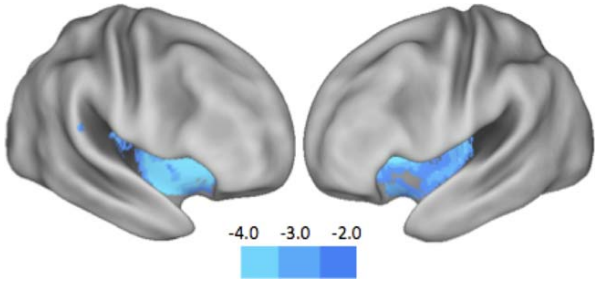

Figure 4.
Results of the voxel-based morphometry analysis. Hallucinators were significantly more likely to suffer from decreased gray matter density in the right anterior insula (peak voxel: 38, 2, −2) and left anterior insula (−32, 16, −8). This suggests that patients with visual misperceptions are unable to use their anterior insula in order to actively recruit activation in the dorsal attention network in the presence of an ambiguous stimulus. Color intensity on the graph represents the *t*-statistic at each voxel after correction for multiple comparisons (FDR $P < 0.05$). [Color figure can be viewed in the online issue, which is available at wileyonlinelibrary.com.]

groups revealed that the hallucinators showed a significant decrease in the inter-network functional connectivity between the DAN and the VAN. Specifically, there were significant negative correlations between the left dorsal anterior cingulate and the left frontal eye fields (difference between Fisher's Z scores (ΔZ) = 0.18, $P < 0.05$), between the right dorsal anterior cingulate and the left frontal eye fields ($\Delta Z = 0.20$, $P < 0.05$) and the right frontal eye fields ($\Delta Z = 0.17$, $P < 0.05$) and between the left AI and the left frontal eye fields ($\Delta Z = 0.20$, $P < 0.05$). Compared with hallucinators, the non-hallucinators also showed a stronger association between the right dorsal anterior cingulate and the left anterior inter-parietal lobule of the DMN ($\Delta Z = 0.13$, $P < 0.05$), suggesting decreased functional connectivity between the VAN and the DMN in hallucinators. In addition, there was a negative correlation between the BPP Error score and the functional connectivity between the left dACC and left FEF ($r = -0.649$, $P < 0.01$), along with the right dACC and the FEF in each hemisphere (left: $r = -0.492$, $P < 0.05$; right: $r = -0.506$, $P < 0.05$).

VBM analysis

After correction for multiple comparisons, hallucinators were significantly more likely to suffer from decreased gray matter density in the right anterior insula (Fig. 4; peak voxel: 38, 2, −2) and the left anterior insula (peak voxel: −32, 16, −8). The volume of gray matter present in the bilateral AI was inversely correlated with BPP Error score ($r = -0.679$, $P < 0.005$; $R^2 = 0.46$), suggesting that a decrease in the gray matter integrity within the anterior insula was associated with worse performance on the BPP (Figs. 5 and 6).

Inter-relation of task-based, rsfcMRI, and VBM analyses

The volume of gray matter within the bilateral anterior insula were positively correlated with the relative BOLD signal within the DAN during the viewing of a bistable

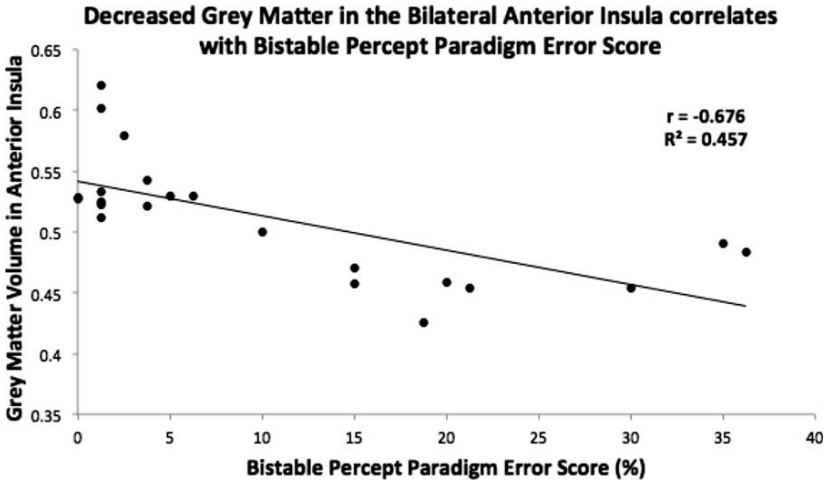

Figure 5.
Results of the voxel-based morphometry analysis. Decreased gray matter density in the bilateral anterior insula was inversely correlated with performance on the bistable percept paradigm ($r = -0.676$, $P < 0.001$; $R^2 = 0.457$), suggesting that gray matter integrity in the bilateral anterior insula is required for adequate performance of the bistable percept paradigm.

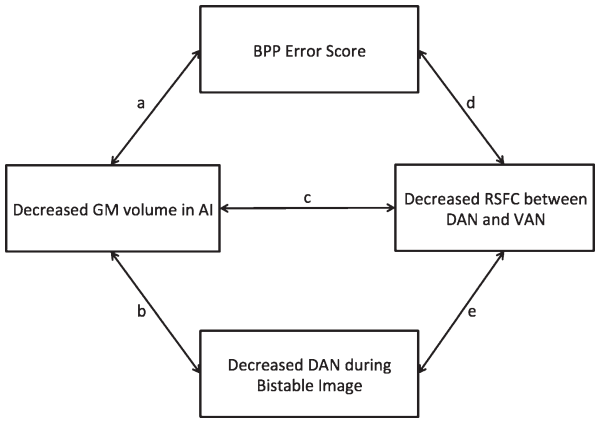

Figure 6.

Inter-relatedness of neuroimaging findings and performance on the bistable percept paradigm. Graphical depiction of the inter-related nature of the findings from the neuroimaging experiments and performance on the Bistable Percept Paradigm (BPP). The strengths of each connection reflect the relative connection between the two measures: (**a**) the volume of gray matter within the bilateral anterior insula (AI) is associated with a lower score on the BPP ($r = -0.679$, $P < 0.005$); (**b**) decreased gray matter in the AI is associated with an inability to recruit the Dorsal Attention Network (DAN) during the viewing of a bistable image ($r = 0.467$, $P < 0.05$); (**c**) decreased gray matter in the AI is also predictive of decreased resting state functional connectivity (RSFC) between hubs of the Ventral Attention Network (VAN) and the DAN ($r = 0.440$, $P < 0.05$); (**d**) there was a negative correlation between the BPP Error score and the functional connectivity between the left dACC and left FEF ($r = -0.649$, $P < 0.01$), along with the right dACC and the bilateral FEF (left: $r = -0.492$, $P < 0.05$; right: $r = -0.506$, $P < 0.05$); and (**e**) the degree of impaired functional connectivity between the VAN and the DAN also predicted the decrease in the BOLD signal in the DAN during the viewing of either a monostable ($r = 0.457$, $P < 0.05$) or a bistable ($r = 0.520$, $P < 0.05$) image.

image ($r = 0.467$, $P < 0.05$), suggesting that patients with less gray matter within the AI were unable to effectively recruit the DAN during the viewing of a bistable image (Fig. 6). This relationship was not present when viewing monostable images.

Reductions in anterior insula gray matter were also predictive of abnormalities in the resting state functional connectivity between regions of the VAN and the DAN (Fig. 6). Specifically, the volume of gray matter in the anterior insula was positively correlated with the functional connectivity between the right dACC and the bilateral FEF (left: $r = 0.440$, $P < 0.05$; right: $r = 0.43$, $P < 0.05$). As such, decreased gray matter integrity in the AI appears to drive a decrease in the connectivity between the DAN and the VAN.

Resting state functional connectivity between the DAN and VAN also predicted the degree of decreased BOLD response within the DAN during the viewing of either a monostable or bistable image (Fig. 6). The average BOLD response in the DAN during the viewing of a monostable image was correlated with the functional connectivity between the right dACC and the right SPL ($r = 0.457$, $P < 0.05$). During the viewing of a bistable image, the BOLD response within the DAN was positively correlated with the degree of connectivity between the right FEF and the bilateral AI (left: $r = 0.520$, $P < 0.05$; right: $r = 0.427$, $P < 0.05$).

DISCUSSION

Utilizing a combination of structural and functional neuroimaging, the major findings of this study are in accordance with the hypothesis that disruption within the attentional networks plays a significant role in the pathophysiology underlying VH in PD. Specifically, our fMRI results demonstrate that hallucinators fail to significantly engage the DAN when processing ambiguous visual stimuli. In addition, analysis of rsfcMRI within the attentional control networks revealed reduced coherence between the DAN and the VAN amongst hallucinators. Finally, hallucinators had a relative loss of gray matter volume within the anterior insula, a key hub within the VAN that facilitates the shifting of attention to the DAN in the presence of ambiguous visual stimuli [Menon and Uddin, 2010; Shine et al., 2011]. Finally, the findings from these three complimentary analyses were all strongly and predictably inter-related (see Fig. 6), thus allowing an internally consistent framework by which the results give insight into the pathophysiology underlying visual misperceptions and hallucinations.

In contrast with previous fMRI studies of VH in PD, we did not see any significant group differences in occipital or temporal extrastriate visual cortices [Ibarretxe-Bilbao et al., 2011], perhaps due to the fact that the two groups in our study were matched for visual acuity and contrast sensitivity. Indeed, there was a consistent recruitment of the occipital cortices during the processing of visual cues in both groups, however, there were significant and relevant differences between the two groups of patients in the neural regions underlying executive functions. Hallucinators showed significantly reduced BOLD activation bilaterally within the frontal eye fields and the superior parietal lobule compared to non-hallucinating patients, regardless of whether they were processing a monostable or bistable image. These regions are both well-described hubs within the putative DAN [Fox et al., 2006], which is an interconnected network of neural centers responsible for processing ambiguous information in the top-down direction of attention. In addition, the BOLD response in the right frontal eye fields was negatively correlated with the percentage of misperceptions, suggesting that poor performance on the BPP was associated with a reduced ability to recruit activation within specific hubs of the DAN.

Furthermore, both groups showed similar patterns of deactivation within the VAN and DMN when processing ambiguous visual stimuli (Fig. 3). However, while non-hallucinators were able to recruit activation in the DAN, hallucinators were not, showing no significant activation of the DAN in the presence of both monostable and bistable percepts.

Hallucinators also showed a relative decrease in BOLD response within the caudal midbrain. This pattern of decreased BOLD signal may reflect an inability to accurately increase neural firing within dopaminergic projection nuclei, such as the substantia nigra and ventral tegmental area, in response to an ambiguous stimulus. Indeed, in conjunction with the central amygdala, the substantia nigra has been shown to underpin the coding of prediction-error and the enhancement of attention in the presence of salient stimuli [Lee et al., 2006]. Alternatively, it is possible that the decreased BOLD response in the midbrain is due to abnormal firing patterns occurring in the nuclei underlying arousal. There is a strong link between the presence of Rapid Eye Movement Sleep Behavior Disorder (RBD) and visual hallucinations [Manni et al., 2011], which might reflect contributions operating through the ascending brainstem arousal system. Indeed, the neuropathology of RBD is presumed to relate to a concentration of Lewy body deposits within specific regions of the midbrain and pons, such as the sublateral dorsal nucleus [Lu et al., 2006].

When comparing the BOLD response pattern to the presentation of monostable and bistable percepts in the cohort of hallucinators, there was a significant increase in neural hubs within the VAN (dACC) and the DMN (HF). However, despite the increased BOLD response seen in these hubs, there was no consistent response across these putative attentional network clusters, perhaps secondary to the small numbers of participants in this experiment. It is not clear from these analyses whether the regions within the VAN and DMN are activating efficiently as entire networks or whether specific hubs within these networks are processing the ambiguous information. The latter interpretation is supported by recent work using spatial and temporal independent component analysis that has shown that individual attentional networks have a number of separate subcomponents (known as temporal functional modes) subserving separate and distinct functions [Smith et al., 2012]. While our study was not designed to explore the data in this manner, such future subanalyses may help to shed light on these speculations.

When exploring the patterns of rsfcMRI within and between the two groups of patients, we saw a specific reduction in the connectivity between the DAN and the VAN in the hallucinators. Specifically, there was significantly decreased connectivity between the bilateral dACC and the AI of the VAN and the left FEF of the DAN. Interestingly, the decreases in these connections were strongly correlated with decreased gray matter volume within the anterior insula as well as the BPP Error Score (Fig. 6). There was also a decrease in the connectivity between the left aIPL of the DMN and left dACC of the VAN, suggesting further internetwork disruption within hallucinators. Interestingly, there were no differences in the intranetwork connectivity between the two groups, with strong intranetwork connections observed in both hallucinators and non-hallucinators. Taken together, these results suggest that an intranetwork pathological process was not likely to be responsible for the impaired communication between the VAN and DAN.

The results from the VBM analysis provide further clues to the underlying pathogenesis of VH in PD. Specifically, hallucinators showed a relative decrease in gray matter volume within the bilateral anterior insula (right $>$ left) when compared with non-hallucinators ($P < 0.05$, FDR corrected). These same regions were found to be active in the entire cohort when comparing the response to bistable $>$ monostable percepts. In addition, the severity of gray matter loss in the anterior insula was strongly correlated with the BPP Error score, as well as impairments in both the resting state and task-based analyses (Figs. 5 and 6). Together, these relationships suggest a strong degree of coherence among the three separate techniques and suggest the possibility of a unified mechanism underlying visual misperceptions in PD.

The results in this study are aligned with previous VBM studies, which have found widespread insula and subcortical gray matter loss in patients with PD and hallucinations [Ibarretxe-Bilbao et al., 2010, 2011; Yamamoto et al., 2007]. However, we did not find any hippocampal atrophy in the hallucinators, perhaps due to a lack of overt dementia in the cohort. In addition, our results are also different from those found in a recent VBM study, which showed that PD patients with hallucinations had decreased gray matter in a targeted exploration of the cholinergic pedunculopontine nucleus as well as the thalamus [Janzen et al., 2012]. However, that study explored gray matter changes in patients with Parkinson's Disease Dementia and Dementia with Lewy Bodies, both of which are conditions that represent a more advanced disease stage, and hence a larger pathological load, than the patients involved in this analysis. This makes a direct comparison between the results of these two studies difficult.

Interestingly, the anterior insula has been previously proposed to underlie the anatomical basis of the ability to "switch" activation between the attentional control networks [Seeley et al., 2007; Shulman et al., 2009]. Specifically, the anterior insula is proposed to act in conjunction with cortical and subcortical hubs (such as the basolateral amygdala) within the VAN to activate the DAN in the presence of environmental salience. Therefore, those individuals with decreased gray matter in the anterior insula may have lost the ability to effectively "switch" their attention in the presence of an ambiguous stimulus, leading to an inability to appropriately activate the DAN.

While the loss of gray matter in the insula may be due to direct pathology, it is also possible that it reflects changes in

other regions of the brain. For instance, the anterior insula may have become disconnected from midbrain projections of either the ventral tegmental area or the basal forebrain nucleus [Goetz et al., 1982, 1998], depriving the anterior insula of modulatory influence from ascending dopaminergic and cholinergic pathways, respectively. Alternatively, the anterior insula may have lost connections with either the basolateral amygdala or the caudate nucleus, both of which have been implicated in the pathophysiology of visual misperceptions in PD [Harding et al., 2002]. To test these speculations, further neuroimaging experiments should seek to explore the white matter connections between these disparate regions to determine whether a structural disconnection may precede the onset of degeneration of the anterior insula. It is also possible that the anterior insula may have become functionally disconnected from the aforementioned regions without any obvious breakdown in structural connection. This interpretation is consistent with the results of the resting state functional connectivity analysis, which showed that while intranetwork connectivity did not differ between groups, there was a significant decrease in the internetwork connectivity between the VAN and the DAN in hallucinators.

The results of this multimodal MRI study support the specific predictions of the recently proposed attentional network hypothesis of visual misperceptions in PD [Shine et al., 2012), along with other hypotheses that implicate attentional dysfunctions in the pathophysiology of VH in PD [Collerton et al., 2005; Diederich et al., 2005; Gallagher et al., 2011]. There are, however, a number of important limitations to the current study. The experiment was conducted in a small group of PD patients and as such, the results should be replicated in a larger cohort of patients to validate the cross-modal analyses performed here. In addition, these experiments could seek to elucidate the BOLD response pattern associated with de novo visual misperceptions, which occur when a patient misperceives a bistable percept in the presence of a monostable image, or seek to clarify the precise role of the interaction between attention and perception [Gallagher et al., 2011]. Future studies should also aim to further delineate the structural and functional connectivity of PD patients with visual misperceptions, using techniques such as independent component analysis or multi voxel pattern analysis. Finally, future neuroimaging studies exploring misperceptions in patients with PD could also manipulate dopaminergic and cholinergic medications in order to determine the precise role of specific neurotransmitters in the pathophysiology of VH. This work may help to uncover mechanisms that may assist in the replacement of normal DAN function in the perception of ambiguous stimuli.

ACKNOWLEDGMENTS

The authors would like to thank Nathan Spreng for his assistance with Caret software and for the graphical depictions of the various attentional networks in Figure 3. They would also like to thank Matthew Brett for his assistance with the processing and interpretation of the region-of-interest analyses. Finally, they would like to thank Parkinson's NSW for their ongoing assistance in support of our research efforts.

REFERENCES

Ashburner J, Friston KJ (2000): Voxel-based morphometry—The methods. NeuroImage 11:805–821.

Asplund CL, Todd JJ, Snyder AP, Marois R (2010): A central role for the lateral prefrontal cortex in goal-directed and stimulus-driven attention. Nat Neurosci 13:507–512.

Beck AT, Steer RA, Brown GK (1996): Manual for the Beck Depression Inventory-II. San Antonio, TX: Psychological Corporation.

Berrios G (1982): Tactile hallucinations: conceptual and historical aspects. J Neurol Neurosurg Psychiatry 45:285–293

Binder JR, Frost JA, Hammeke TA, Bellgowan PS, Rao SM, Cox RW (1999): Conceptual processing during the conscious resting state: A functional MRI study. J Cognit Neurosci 11:80–93.

Brett M, Anton J, Valabregue R, Poline J (2002): Region of interest analysis using an SPM toolbox [abstract]. Presented at the 8th International Conference on Functional Mapping of the Human Brain. Neuroimage 16(2).

Bronnick K, Aarsland D, Larsen JP (2005): Neuropsychiatric disturbances in Parkinson's disease clusters in five groups with different prevalence of dementia. Acta Psychiatr Scand 112:201–207.

Collerton D, Perry E, McKieth I (2005): When people see things that are not there: A novel perception and attention deficit model of recurrent complex visual hallucinations. Behav Brain Sci 28:737–757.

Corbetta M, Shulman GL (2002): Control of goal-directed and stimulus-driven attention in the brain. Nat Rev Neurosci 3:201–215.

Corrigan J, Hinkeldey MS (1987): Relationships between parts A and B of the Trail Making Test. J Clin Psychol 43:402–409.

Diederich NJ, Goetz CG, Raman R, Pappert EJ, Leurgans S, Piery V (1998): Poor visual discrimination and visual hallucinations in Parkinson's disease. Clin Neuropharmacol 21:289–295.

Diederich NJ, Goetz CG, Stebbins GT (2005): Repeated visual hallucinations in Parkinson's disease as disturbed external/internal perceptions: Focused review and a new integrative model. Mov Disord 20:130–140.

Diederich NJ, Fenelon G, Stebbins G, Goetz CG (2009): Hallucinations in Parkinson disease. Nat Rev Neurol 5:331–342.

Elliot DB, Sanderson K, Conkey A (1990): The reliability of the Pelli-Robson contrast sensitivity chart. Ophthalmic Physiol Opt 10:21–24.

Emre M, Aarsland D, Brown R, Burn DJ, Duyckaerts C, Mizuno Y, Broe GA, Cummings J, Dickson DW, Gauthier S, Goldman J, Goetz C, Korczyn A, Lees A, Levy R, Litvan I, McKeith I, Olanow W, Poewe W, Quinn N, Sampaio C, Tolosa E, Dubois B. (2007): Clinical diagnostic criteria for dementia associated with parkinson's disease. Mov Disord 22:1689–1707.

Fenelon G, Mahieux F, Huon R, Ziegler M (2000): Hallucinations in parkinson's disease: Prevalence, phenomenology and risk factors. Brain 124:733–745.

Forsaa EB, Larsen JP, Wentzel-Larsen T, Goetz CG, Stebbins GT, Aarsland D, Alves G. (2010): A 12-year population-based study of psychosis in parkinson disease. Arch Neurol 67:996–1001.

Fox MD, Snyder AZ, Vincent JL, Corbetta M, Van Essen DC, Raichle ME (2005): The human brain is intrinsically organized into dynamic, anticorrelated functional networks. Proc Natl Acad Sci USA 102:9673–9678.

Fox MD, Corbetta M, Snyder AZ, Vincent JL, Raichle ME (2006): Spontaneous neuronal activity distinguishes human dorsal and ventral attention systems. Proc Natl Acad Sci USA 103:10046–10051.

Gagnon JF, Postuma RB, Joncas S, Desjardins C, Latreille V (2010): The montreal cognitive assessment: A screening tool for mild cognitive impairment in REM sleep behavior disorder. Mov Disord 2010;25:936–940.

Gallagher DA, Parkkinen L, O'Sullivan SS, Sprat A, Shah A, Davey CC, Bremner FD, Revesz T, Williams DR, Lees AJ, Schrag A. (2011): Testing an aetiological model of visual hallucinations in Parkinson's disease. Brain 134:3299–3309.

Goetz CG, Tanner C, Klawans H (1982): Pharmacology of hallucinations induced by long-term drug therapy. Am J Psychiatry 139:494–497.

Goetz CG, Vogel C, Tanner CM, Stebbins GT (1998): Early dopaminergic drug-induced hallucinations in parkinsonian patients. Neurology 51:811–814.

Goetz C, Fan W, Leurgans S, Bernard B, Stebbins G (2006): The malignant course 'benign hallucinations' in Parkinson's disease. Arch Neurol 2006;63:713–716.

Goetz CG, Fahn S, Martinez-Martin P, Poewe W, Sampaio C, Stebbins GT, Stern MB, Tilley BC, Dodel R, Dubois B, Holloway R, Jankovic J, Kulisevsky J, Lang AE, Lees A, Leurgans S, LeWitt PA, Nyenhuis D, Olanow CW, Rascol O, Schrag A, Teresi JA, van Hilten JJ, and LaPelle N (2007): Movement Disorder Society-Sponsored Revision of the Unifited Parkinson's Disease Rating Scale (MDS-UPDRS): Process, Format, and Clinimetric Testing Plan. Mov Disord 22:41–47.

Harding AJ, Stimson E, Henderson JM, Halliday GM (2002): Clinical correlates of selective pathology in the amygdala of patients with Parkinson's disease. Brain 125 (Part 11):2431–2445.

Honey CJ, Sporns O, Cammoun L, Gigandet X, Thiran JP, Meuli R, Hagmann P. (2009): Predicting human resting-state functional connectivity from structural connectivity. Proc Natl Acad Sci USA 106:2035–2040.

Horwitz B, Warner B, Fitzer J, Tagamets MA, Husain FT, Long TW (2005): Investigating the neural basis for funcational and effective connectivity. Application to fMRI. Philos Trans R Soc Lond B Biol Sci 360:1093–1108.

Ibarretxe-Bilbao N, Ramirez-Ruiz B, Junque C, Marti MJ, Valldeoriola F, Bargallo N, Juanes S, et al. (2010): Differential progression of brain atrophy in Parkinson's disease with and without visual hallucinations. J Neurol Neurosurg Psychiatry 81:650–657.

Ibarretxe-Bilbao N, Junque C, Marti MJ, Tolosa E (2011): Cerebral basis of visual hallucinations in Parkinson's disease: Structural and functional MRI studies. Neurol Sci 310:79–81.

Janzen J, van't Ent D, Lemstra AW, Berendse HW, Barkhof F, Foncke EMJ (2012): The pedunculopontine nucleus is related to visual hallucinations in Parkinson's disease: Preliminary results of a voxel-based morphometry study. J Neurol 259:147–154.

Lee HJ, Youn JM, Mary JO, Gallagher M, Holland PC (2006): Role of substantia nigra-amygdala connections in surprise-induced enhancement of attention. J Neurosci 26:6077–6081.

Lewis SJG, Shine JM, Duffy S, Halliday GM, Naismith SL (2012): Anterior cingulate integrity: Executive and neuropsychiatric features in parkinson's disease. Mov Disord 27:1262–1267.

Llebaria Gm Pagonabarraga J, Martinez-Corral M, Garcia-Sanchez C, Pascual-Sedano B, Gironell A, Kulisevsky J (2010): Neuropsychological correlates of mild to severe hallucinations in Parkinson's disease. Mov Disord 25:2785–2791.

Lu J, Sherman D, Devor M, Saper CB (2006): A putative flip-flop switch for control of REM sleep. Nature 441:589–594.

Mazaika PK, Whitfield S, Cooper JC (2005): Detection and repair of transient artifacts in fMRI data. NeuroImage 26:S36.

Manni R, Terzaghi M, Ratti PL, Repetto A, Zangaglia R, Pacchettim C (2011): Hallucinations and REM sleep behavior disorder in Parkinson's disease: Dream imagery intrusions and other hypotheses. Conscious Cogn 20:1021–1026.

Martinez-Martin P, Falup-Pecurariu C, Rodriguez-Blazquez C, Serranoduenas M, Carod Artal FJ, Rojo Abuin JM, Aarsland D.. (2011): Dementia associated with Parkinson's disease: Applying the movement disorder society task force criteria. Parkinsonism Relat Disord 17:621–624.

Mazoyer B, Zago L, Mellet E, Bricogne S, Etard O, Houdé O, Crivelo F, Joliot M, Petit L, Tzourio-Mazoyer N. (2001): Cortical networks for working memory and executive functions sustain the conscious resting state in man. Brain Res Bull 54:287–298.

Menon V, Uddin LQ (2010): Saliency, switching, attention and control: A network model of insula function. Brain Struct Funct 214:655–667.

Meppelink AM, de Jong BM, Renken R, Leenders KL, Cornelissen FW, van Laar T (2009): Impaired visual processing preceding image recognition in Parkinson's disease patients with visual hallucinations. Brain 132:2980–2993.

Naismith SL, Shine JM, Lewis SJG (2010): The specific contributions of set-shifting to freezing of gait in Parkinson's disease. Mov Disord 25:1000–1004.

Nomura T, Inoue Y, Mitani H, Kawahara R, Miyake M, Nakashima K (2003): Visual hallucinations as REM sleep behavior disorders in patients with Parkinson's disease. Mov Disord 18:812–817.

Pieri V, Diederich NJ, Raman R, Goetz CG (2000): Decreased color discrimination and contrast sensitivity in Parkinson's disease. J Neurol Sci 172:7–11.

Price MJ, Feldman RG, Adelberg D, Kayne H (1992): Abnormalities in color vision and contrast sensitivity in Parkinson's disease. Neurology 42:887.

Ramírez-Ruiz B, Martí MJ, Tolosa E, Gimenez M, Bargallo N, Vakkdeiruika F, Junque C. (2007): Cerebral atrophy in Parkinson's disease patients with visual hallucinations. Eur J Neurol 14:750–756.

Sanchez-Ramos JR, Ortoll R, Paulson GW (1996): Visual hallucinations associated with parkinson disease. Arch Neurol 53:1265–1268.

Sanchez-Castaneda C, Rene R, Ramirez-Ruiz B, Campdelacreu J, Gascon J, Falcon C, Calopa M, Jauma S, Juncadella M, Junque C. (2010): Frontal and associative visual areas related to visual hallucinations in dementia with Lewy bodies and Parkinson's disease with dementia. Mov Disord 25:615–622.

Scaglione C, Vignatelli L, Piazzi G, Marchese R, Negrotti A, Rizzo G, Lopane G, Bassein L, Maestri M, Bernardini S, Martinelli P, Abbruzzese G, Calzetti S, Bonuccelli U, Provini F, Coccagna G;

Bologna, Genova, Parma and Pisa Universities group for the study of REM Sleep Behavior Disorder in Parkinson's Disease. (2005): REM sleep behavior disorder in Parkinson's disease: A questionnaire-based study. Neurol Sci 25:316–321.

Seeley WW, Menon V, Schatzberg AF, Keller J, Glover GH, Kenna H, Reiss AL, Grecius MD. (2007): Dissociable intrinsic connectivity networks for salience processing and executive control. J Neurosci 27:2349–2356.

Shine JM, Halliday GM, Naismith SL, Lewis SJG (2011): Visual misperceptions and hallucinations in Parkinson's disease: Dysfunction of attentional control networks? Mov Disord 26:2154–2159.

Shine JM, Halliday GM, Carlos M, Naismith SL, Lewis SJG (2012): Investigating visual misperceptions in Parkinson's disease: A novel behavioral paradigm. Mov Disord 27:500–505.

Shulman GL, Astafiev SV, Franke D, Pope DLW, Snyder AZ, McAvoy MP, et al. (2009): Interaction of stimulus-driven reorienting and expectation in ventral and dorsal fronto-parietal and basal ganglia-cortical networks. J Neurosci 29:4392–4407.

Sporns O (2011): Networks of the Brain, 1st ed. MIT Press, Cambridge MA.

Smith SM, Miller KL, Moeller S, Xu J, Auerbach EJ, Woolrich MW, et al. (2012): Temporally-independent functional modes of spontaneous brain activity. Proc Natl Acad Sci USA 109:3131–3136.

Spreng RN, Stevens WS, Chamberlain JP, Gillmore AW, Schacter DL (2010): Default network activity, coupled with the frontoparietal control network, supports goal-directed cognition. Neuroimage 53:303–317.

Stebbins GT, Goetz CG, Carrillo MC, Bangen KJ, Turner DA, Glover GH, Gabrieli J. (2004): Altered cortical visual processing in PD with hallucinations: An fMRI study. Neurology 63:1409–1416.

Uchiyama M, Nishio Y, Yokoi K, Hirayama K, Imamura T, Shimomura T, Mori E. (2012): Pareidolias: Complex visual illusions in dementia with Lewy bodies. Brain 135:2458–24693.

Van den Heuvel MP, Hulshoff Pol HE (2010): Exploring the brain network: A review on resting-state fMRI functional connectivity. Eur Neuropsychopharmacol 20:519–534.

Visser M, Verbaan D, van Rooden SM, Stiggelbout AM, Marinus J, van Hilten JJ (2007): Assessment of psychiatric complications in Parkinson's disease: The SCOPA-PC. Mov Disord 22:2221–2228.

Yamamoto R, Iseki E, Murayama N, Minegishi M, Marui W, Togo T, Katsuse O, Kosaka K, Kato M, Iwatsubo T, Arai H (2007): Correlation in Lewy pathology between the claustrum and visual areas in brains of dementia with Lewy bodies. Neurosci Lett 415:219–224.